Design, synthesis and in vitro antitumor activity of novel N-substituted-4-phenyl/benzylphthalazin-1-ones

ARTICLE *in* EUROPEAN JOURNAL OF MEDICINAL CHEMISTRY · OCTOBER 2014

Impact Factor: 3.45 · DOI: 10.1016/j.ejmech.2014.10.064

5 AUTHORS, INCLUDING:

Wagdy M. Eldehna
Egyptian Russian University
13 PUBLICATIONS **25** CITATIONS
SEE PROFILE

Hany S. Ibrahim
Egyptian Russian University
12 PUBLICATIONS **33** CITATIONS
SEE PROFILE

Hatem Abdel-Aziz
National Research Center, Egypt
159 PUBLICATIONS **998** CITATIONS
SEE PROFILE

Mohieldin Youssef
The American University in Cairo
3 PUBLICATIONS **10** CITATIONS
SEE PROFILE

European Journal of Medicinal Chemistry 89 (2015) 549–560

Contents lists available at ScienceDirect

European Journal of Medicinal Chemistry

journal homepage: http://www.elsevier.com/locate/ejmech

Original article

Design, synthesis and *in vitro* antitumor activity of novel *N*-substituted-4-phenyl/benzylphthalazin-1-ones

Wagdy M. Eldehna [a, *], Hany S. Ibrahim [a], Hatem A. Abdel-Aziz [b, c, **], Noha N. Farrag [d], Mohieldin M. Youssef [d, e]

[a] Department of Pharmaceutical Chemistry, College of Pharmacy, Egyptian Russian University, P.O. Box 11829, Badr City, Cairo, Egypt
[b] Department of Pharmaceutical Chemistry, College of Pharmacy, King Saud University, P.O. Box 2457, Riyadh 11451, Saudi Arabia
[c] Department of Applied Organic Chemistry, National Research Center, P.O. Box 12622, Dokki, Giza, Egypt
[d] Department of Biology, School of Sciences and Engineering (SSE), The American University in Cairo, P.O. Box 11835, New Cairo, Egypt
[e] Department of Pharmacology and Toxicology, College of Pharmacy, Egyptian Russian University, Badr City, Cairo, P.O. Box 11829, Egypt

ARTICLE INFO

Article history:
Received 12 June 2014
Received in revised form
7 October 2014
Accepted 22 October 2014
Available online 23 October 2014

Keywords:
Phthalazin-1-one
Antitumor activity
HepG2
Apoptosis

ABSTRACT

A novel series of *N*-substituted-4-phenylphthalazin-1-ones **14a**–**g** bearing different anilines at the N-2 of phthalazin-1-one scaffold *via* acetyl-flexible linker was designed and synthesized for the development of potential anticancer agents. Compounds **19a**–**g** were synthesized by insertion of methylene (CH_2) bridge at C4-position of **14a**–**g** to provide a flexibility for the phenyl group. The newly synthesized compounds **14a**–**g** and **19a**–**g** were evaluated for their anti-proliferative activity against three human tumor cell lines HepG2 hepatocellular carcinoma, HT-29 colon cancer and MCF-7 breast cancer. In particular, HepG2 and HT-29 cancer cell lines were more susceptible to the synthesized derivatives. Compound **19d** ($IC_{50} = 1.2 \pm 0.09$ μM) was found to be the most potent derivative against HepG2 as it was 2.9 times more active than doxorubicin ($IC_{50} = 3.45 \pm 0.54$) and sorafenib ($IC_{50} = 3.5 \pm 1.04$ μM). Compounds **14e**, **14g**, **19d** and **19g** with $IC_{50} = (3.29 \pm 0.45)$, (3.50 ± 0.846), (1.20 ± 0.09) and (3.52 ± 0.70) μM, respectively, were found to be active candidates against HepG2 cancer cells. Compounds **14e**, **14g**, **19d** and **19g** were able to induce apoptosis in HepG2, this was assured by; the significant increase in the percentage of annexin V–FITC-positive apoptotic cells (UR + LR), the down-regulation of the anti-apoptotic protein Bcl-2 and the up-regulation of the pro-apoptotic protein Bax, in addition to boosting caspase-3 levels. Moreover, cytotoxicity evaluation of the newly synthesized compounds in HT-29 revealed that compounds **14e**, **14f**, **19e** and **19f** ($IC_{50} = 3.05 \pm 0.78$, 4.02 ± 1.18, 3.68 ± 0.79 and 2.98 ± 0.47 μM, respectively) were more potent than doxorubicin ($IC_{50} = 7.70 \pm 1.78$ μM).

1. Introduction

Cancer is one of the most difficult diseases to treat and it is a major disease responsible for deaths worldwide, it can be considered as one of the foremost health problems [1]. Yet there is no cancer treatment that is 100% effective against disseminated cancer [2]. Therefore, there is an urgent need to give much attention to update and modify drug leads from the point of view of medicinal chemistry and drug design to fulfill more potent and effective therapies.

On the other hand, phthalazine nucleus has been emerged as a promising and attractive scaffold in the development of potent antitumor agents. For example, phthalazin-1,4-diones have been reported as potent type II IMP dehydrogenase inhibitors [3] and as effective anti-proliferative agents against different human and murine tumor cells [4,5] particularly against hepatocellular carcinoma [6]. In addition, 1,4-disubstituted phthalazines have been emerged as promising and attractive antitumor agents. For example, 1-piperazinyl-4-substitutedphthalazines have been reported as active cytotoxic agents against A549, HT-29 and MDA-MB-231 [7–9] whereas 1-anilino-4-(arylsulfanylmethyl)phthalazines showed an interesting cytotoxic activity against Bel-7402 and HT-1080 [10,11]. Moreover, *Novartis* identified a new class of Hedgehog (Hh) pathway inhibitors which acts *via* antagonism of the smoothened receptor with a main structure of 1-piperazinyl-4-benzylphthalazine [12] while *Amgen* has reported in two studies

* Corresponding author.
** Corresponding author. Department of Pharmaceutical Chemistry, College of Pharmacy, King Saud University, P.O. Box 2457, Riyadh 11451, Saudi Arabia.
E-mail addresses: wagdy2000@gmail.com (W.M. Eldehna), hatem_741@yahoo.com (H.A. Abdel-Aziz).

http://dx.doi.org/10.1016/j.ejmech.2014.10.064
0223-5234/

the design of 1-piperazinyl-4-arylphthalazines as potent smoothened antagonists [13,14].

During the last two decades there is a growing interest in the synthesis of several phthalazines as promising drug candidates for the treatment of cancer. The latter research efforts have led to the discovery of several leading phthalazines with different cellular and enzymatic targets. For example, AMG 900 **1** (Fig. 1) was synthesized by *Amgen* as orally bioavailable, potent, and highly selective pan-aurora kinase inhibitor that is active in taxane-resistant tumor cell lines [15]. AMG 900 **1** was active in an AZD1152-resistant HCT116 variant cell line that harbors an aurora-B mutation (*W221L*) [16]. Thereafter, Cee et al. have discovered two selective and orally bioavailable pyridinyl-pyrimidine phthalazines aurora kinase inhibitors [17].

Vatalanib (PTK787) **2** [18] (Fig. 1) inhibits both VEGFR-1 and VEGFR-2 with IC_{50} of 380 and 20 nM, respectively. Vatalanib **2** is well absorbed orally and shows *in vivo* antitumor activity against a panel of human tumor xenograft models, however, vatalanib **2** is currently in phase III clinical trials for the treatment of colorectal cancer [19,20]. In addition, many anilino-phthalazines, have been reported as potent inhibitors of VEGFR-2 as AAC789 **3** and IM-023911 **4** with IC_{50} = 20 and 48 nM, respectively (Fig. 1) [21–26].

Inhibitors of PARPs family of proteins are currently being evaluated as potential anticancer medicines at both preclinical and

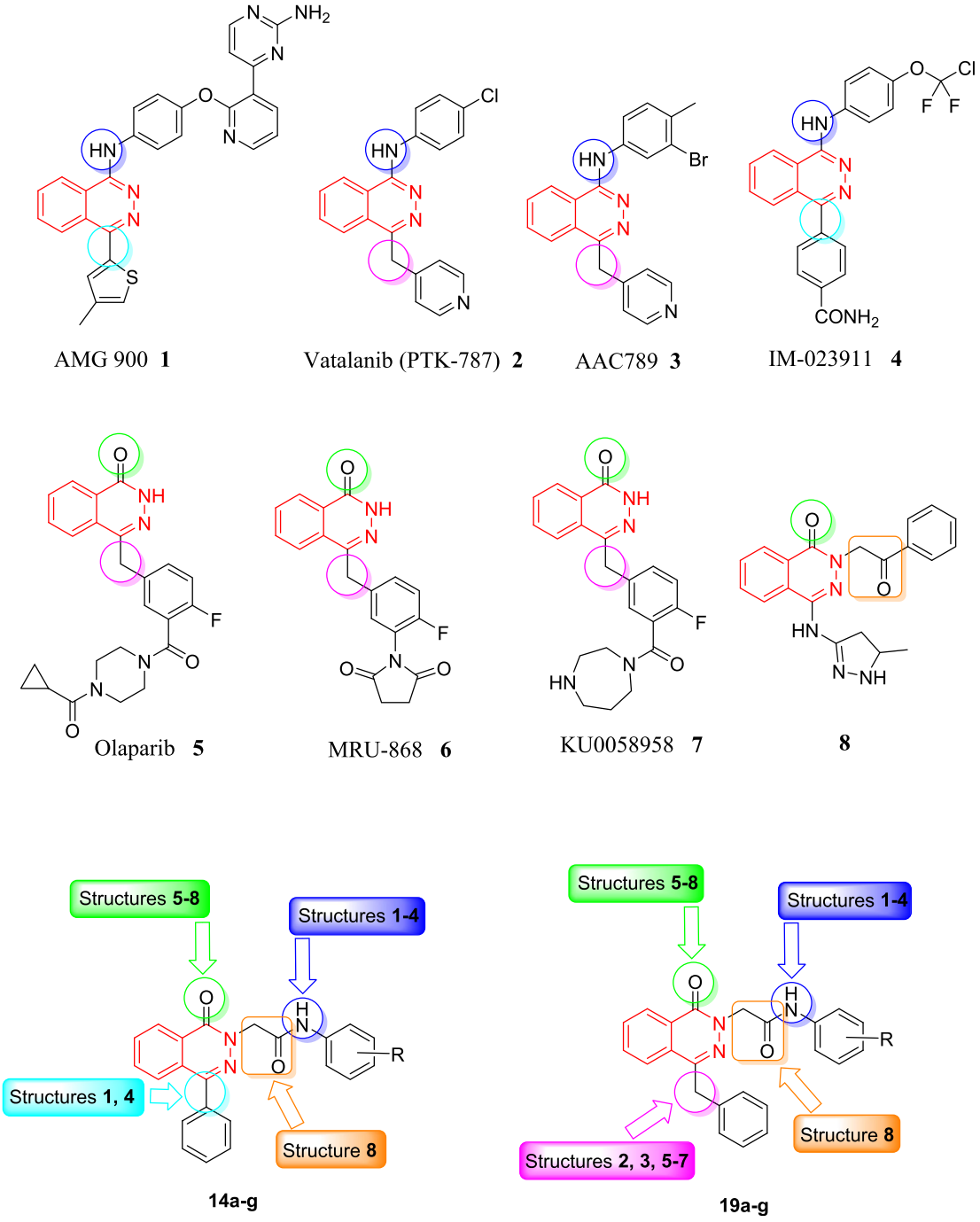

Fig. 1. Structure of the lead anticancer phthalazine derivatives **1**–**8** and the designed target phthalazinones **14a**–**g** and **19a**–**g**.

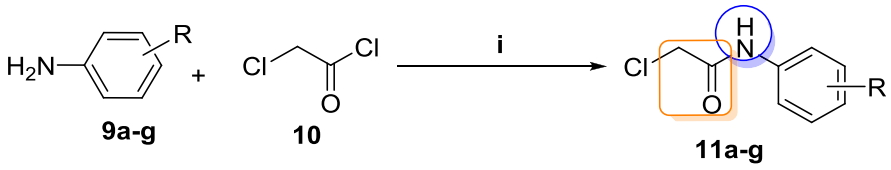

11, a = H, **b** = 4-OCH_3, **c** = 4-F, **d** = 2-Cl, **e** = 3-Cl, **f** = 4-Cl, **g** = 3-CF_3

Scheme 1. Reagents and conditions: (i) dioxan/0 °C, 1 h, then rt 2 h.

clinical levels [27]. A series of 4-substituted-2*H*-phthalazin-1-ones have been investigated as potent orally bioavailable PARP inhibitor [28–30]. Olaparib **5**, MRU-868 **6** and KU0058958 **7** are the most interesting PARP inhibitors based on the 4-substituted-2*H*-phthalazin-1-one scaffold, for example, olaparib **5** is a single digit nanomolar inhibitor of both PARP-1 and PARP-2 that shows standalone activity against BRCA1-deficient breast cancer cell lines.

Interestingly, Prime et al. have reported a novel class of potent, selective, and orally bioavailable inhibitors of aurora-A kinase based upon a 4-(pyrazole-3-ylamino)phenyl-2*H*-phthalazin-1-one scaffold. Compound **8** inhibits aurora-A with IC_{50} of 71 nM, also, it showed *in vitro* cytotoxic activity against HCT116 colon cell line with IC_{50} of 5.44 μM [31].

In view of the facts mentioned above, the majority of the reported studies were concerned with C-1 or C-4 substituted phthalazines whereas a little attention was given to investigate SAR of N-2 substituted phthalazines. This has inspired the present study to design a series of new N-2 substituted phthalazines in an attempt to obtain a potent anticancer agent. The strategy adopted included moving the anilino moiety of compounds **1**–**4** from C-1 to N-2 of phthalazine moiety. The flexible acetyl linker (–CH_2CO–) of **8** was selected to link the anilino moiety to the phthalazine core. In the target phthalazines **14a**–**g**, phenyl group was selected to substitute the C-4 of the phthalazine core. Utilization of benzyl group to substitute the C-4, as in case of structures **2**, **3**, **5**–**7**, was performed in target compounds **19a**–**g** to carry out further elaboration of the phthalazinone scaffold and to explore a valuable SAR (Fig. 1). The latter designed target phthalazinones **14a**–**g** and **19a**–**g** were synthesized to evaluate their anti-tumor activity against three human tumor cell lines, namely, HepG2 hepatocellular carcinoma, HT-29 colon cancer and MCF-7 breast cancer.

2. Results and discussion

2.1. Chemistry

The route adopted for the preparation of the new phthalazine derivatives is depicted in Schemes 1–3. The amino function of the selected anilines was acylated with 2-chloroacetyl chloride in cold dioxan to furnish the key intermediates **11a**–**g** (Scheme 1).

Cyclocondensation of 2-benzoylbenzoic acid (**12**) with refluxing hydrazine sulfate and sodium hydroxide gave 4-phenyl-1(2*H*)-phthalazinone (**13**). The latter compound **13** was reacted with the key intermediates **11a**–**g** in dry refluxing acetone in the presence of potassium carbonate to afford the first series of the target compounds **14a**–**g** (Scheme 2).

The IR spectra of compounds **14a**–**g** showed absorption bands around 3260 cm^{-1} for NH in addition to the absorption bands of carbonyl groups in the region 1659–1692 cm^{-1}. On the other hand the ^{1}H NMR spectra of **14a**–**g** showed the signals of the aliphatic $COCH_2$ protons at a δ range 5.00–5.11 ppm also, ^{1}H NMR spectra revealed the presence of D_2O exchangable NH protons in the range δ 9.89–10.66 ppm. Moreover, their ^{1}H NMR spectra lacked the signal of the acidic NH of **13** which resonate at δ 12.84 ppm. The ^{13}C NMR spectra of **14a**–**g** showed two signals resonating in the range δ 54.07–54.46 ppm and δ 164.99–166.19 ppm attributable for CH_2 and C=O carbons, respectively.

On the other hand, the reaction of phthalic anhydride (**15**) with phenylacetic acid (**16**) in the presence of fused sodium acetate yielded 3-benzalphthalide **17**. Next, cyclocondensation of **17** with hydrazine sulfate and sodium hydroxide was achieved to furnish 4-benzylphthalazin-1(2*H*)-one (**18**). Finally, the second group of the target phthalazinones **19a**–**g** was synthesized by the reaction of the key intermediates **11a**–**g** with 4-benzylphthalazin-1(2*H*)-one (**18**) in dry acetone in the presence of potassium carbonate under reflux temperature.

The IR spectra of the target compounds **19a**–**g** confirmed the presence of the characteristic carbonyl absorption bands around 1650 cm^{-1} and NH absorption bands around 3270 cm^{-1}. On the other hand the ^{1}H NMR spectra of **19a**–**g** showed the singlet signals of the aliphatic $COCH_2$ protons in the range δ 4.96–5.08 ppm, while the benzylic CH_2 protons of **19a**–**g** appeared as singlet signals at δ 4.33 ppm. Furthermore, ^{1}H NMR spectra of these compounds showed a D_2O-exchangeable signal of an NH proton in the region δ 9.81–10.66 ppm. The ^{13}C NMR spectra of **19a**–**g** showed signals resonating in the range δ 53.77–54.20 ppm attributable for the

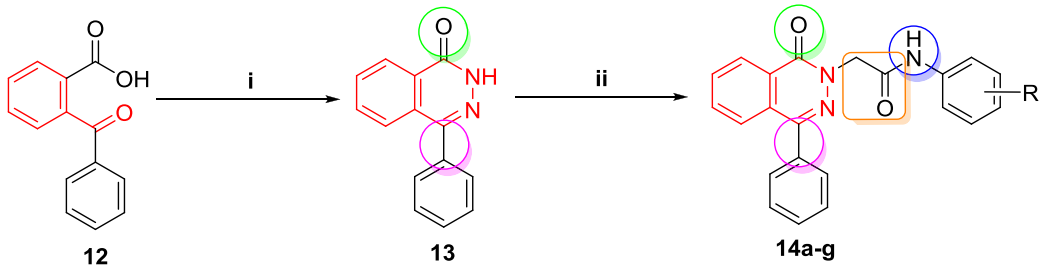

14, a = H, **b** = 4-OCH_3, **c** = 4-F, **d** = 2-Cl, **e** = 3-Cl, **f** = 4-Cl, **g** = 3-CF_3

Scheme 2. Reagents and conditions: (i) $NH_2NH_2.H_2SO_4$/NaOH/reflux 1 h; (ii) **11a**–**g**/acetone/K_2CO_3/KI/reflux 11 h.

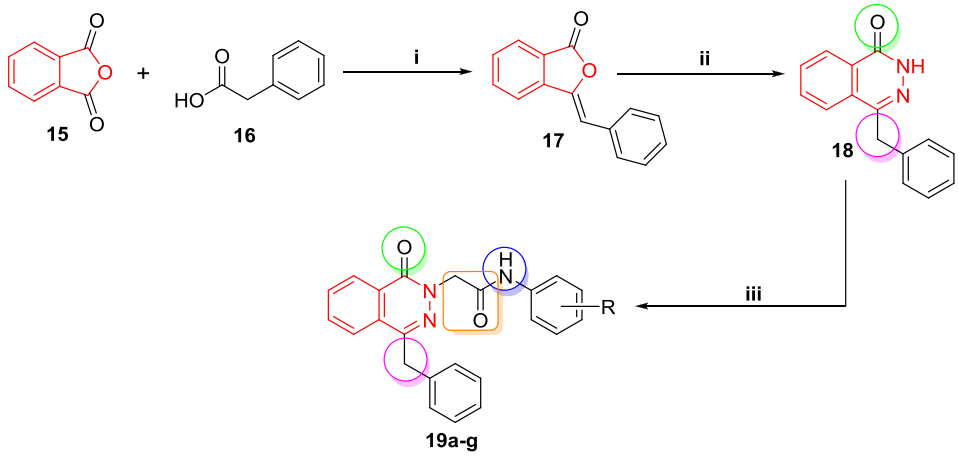

19, a = H, **b** = 4-OCH_3, **c** = 4-F, **d** = 2-Cl, **e** = 3-Cl, **f** = 4-Cl, **g** = 3-CF_3

Scheme 3. Reagents and conditions: (i) CH_3COONa/heating 240 °C, 4 h; (ii) $NH_2NH_2.H_2SO_4$/NaOH/EtOH/heating 95 °C, 15 h; (iii) **11a**–**g**/acetone/K_2CO_3/KI/reflux 9 h.

aliphatic carbons of the acetyl linker while the carbons of carbonyl groups appeared in the range δ 165.57–166.36 ppm. Besides, their ^{13}C NMR spectra showed the signals of the benzylic methylene carbons around δ 37.56 ppm.

2.2. Biological evaluation

2.2.1. In vitro cytotoxic activity

Anti-proliferative activity of the newly synthesized phthalazinones **14a**–**g** and **19a**–**g** was examined in three human cancer cell lines, namely, HepG2 hepatocellular carcinoma, HT-29 colon cancer and MCF-7 breast cancer using sulforhodamine B (SRB) colorimetric assay as described by Skehan et al. [32]. Doxorubicin was included in the experiments as a reference cytotoxic compound for the three cell lines while sorafenib was used as a positive control for HepG2 cancer cells only. The results were expressed as growth inhibitory concentration (IC_{50}) values which represent the compound concentrations required to produce a 50% inhibition of cell growth after 72 h of incubation compared to untreated controls (Table 1).

From the obtained results, it was explicated that most of the prepared compounds displayed excellent to modest growth inhibitory activity against the tested cancer cell lines. Investigations of the cytotoxic activity against HepG2 indicated that it was the most sensitive cell line to the influence of the new derivatives. Compound **19d** (IC_{50} = 1.2 ± 0.09 μM) was found to be the most potent derivative overall the tested compounds against HepG2 as it was 2.9 times more active than doxorubicin (IC_{50} = 3.45 ± 0.54) and sorafenib (IC_{50} = 3.5 ± 1.04 μM). Besides, compounds **14e**, **14g** and **19g** with (IC_{50} = 3.29 ± 0.45, 3.5 ± 0.846 and 3.52 ± 0.70 μM, respectively), were almost equipotent as doxorubicin and sorafenib. Also, compounds **14a**, **14c**, **14d**, **14f**, **19c** and **19e** were moderately active with (IC_{50} of 13.44 ± 2.30, 10.6 ± 1.64, 33.0 ± 3.041, 10.26±, 27.0 ± 2.05 and 14.27 ± 1.28 μM, respectively). On the other hand, cytotoxicity evaluation in HT-29 cell line revealed that compounds **14e**, **14f**, **19e** and **19f** (IC_{50} = 3.05 ± 0.78, 4.02 ± 1.18, 3.68 ± 0.79 and 2.98 ± 0.47 μM, respectively) were more potent and efficacious than doxorubicin (IC_{50} = 7.70 ± 1.78 μM). Whilst, compounds **14c**, **14g** and **19d** with (IC_{50} = 46.24 ± 2.34, 41.19 ± 3.91 and 42.76 ± 4.50 μM, respectively) displayed moderate cytotoxicity compared to doxorubicin. Concerning activity against MCF-7, the first series **14a**–**g** elicited weak potency in this cell type (IC_{50} = 30.0 ± 1.42–77.0 ± 9.54 μM) whereas three members of the second series **19e**–**g** showed moderate activity with (IC_{50} = 10.8 ± 0.85, 13.0 ± 0.764 and 3.85 ± 0.07 μM, respectively).

Table 1
In vitro cytotoxic activities of the newly synthesized compounds against HepG-2, HT-29 and MCF-7 cell lines.

Compound	R	IC_{50} (μM)[a]		
		HepG2	**HT-29**	**MCF-7**
14a	H	13.44 ± 2.30	99 ± 9.05	43.0 ± 6.74
14b	4-OCH_3	NA[b]	NA[b]	77.0 ± 9.54
14c	4-F	10.6 ± 1.64	46.24 ± 2.34	35.0 ± 2.72
14d	2-Cl	33.0 ± 3.041	88.57 ± 6.712	30.0 ± 1.42
14e	3-Cl	3.29 ± 0.45	3.05 ± 0.78	74.0 ± 3.62
14f	4-Cl	10.26 ± 1.05	4.02 ± 1.18	33.0 ± 2.59
14g	3-CF_3	3.5 ± 0.846	41.19 ± 3.91	58.0 ± 4.806
19a	H	66.0 ± 4.178	95.35 ± 6.589	36.0 ± 3.04
19b	4-OCH_3	69.0 ± 3.643	NA[b]	62.0 ± 4.362
19c	4-F	27.0 ± 2.05	98.0 ± 8.066	30.0 ± 2.10
19d	2-Cl	1.2 ± 0.09	42.76 ± 4.50	89.0 ± 7.16
19e	3-Cl	14.27 ± 1.28	3.68 ± 0.79	10.8 ± 0.85
19f	4-Cl	NA[b]	2.98 ± 0.47	13.0 ± 0.764
19g	3-CF_3	3.52 ± 0.70	60.98 ± 6.54	3.85 ± 0.96
Doxorubicin		3.45 ± 0.54	7.7 ± 1.78	1.17 ± 0.07
Sorafenib		3.5 ± 1.04		

[a] IC_{50} values are the mean ± S.D. of three separate experiments.
[b] NA: Compounds having IC_{50} value >100 mM.

2.2.2. Structure activity relationship SAR

The preliminary SAR study has focused on the effect of replacement of the phenyl group at position 4 of the phthalazine scaffold by a benzyl group, on the antitumor activities of the synthesized compounds. In a comparison of the cytotoxic activities of the two series (**14a**–**g** and **19a**–**g**) against hepatic and colon cancer, we found that introduction of this modification has maintained the IC_{50} values within the same ranges whilst, with respect to the breast cancer, the IC_{50} values of the first series members **14a**, **14b**, **14c**, **14e**, **14f** and **14g** (43.0 ± 6.74, 77.0 ± 9.54, 35.0 ± 2.72, 74.0 ± 3.62, 33.0 ± 2.59 and 58.0 ± 4.806 μM, respectively) were decreased to (36.0 ± 3.04, 62.0 ± 4.362, 30.0 ± 1.42, 10.8 ± 0.85, 13.0 ± 0.764 and 3.85 ± 0.96 μM) for their corresponding members in the second series, implying that the replacement of the 4-phenyl group by the benzyl one was indispensable for the activities against breast cancer.

Further investigation of the impact of the substitution pattern of the anilino moiety on the prepared phthalazinones activities was then conducted. Incorporation of unsubstituted anilino moiety has

rendered the compounds **14a** and **19a** with moderate to fair cytotoxic activities against the three tumor cell types. Since fluorine has a size and electronic properties similar to those of hydrogen, it is introduced as an isosteric to the hydrogen atom. Compounds **14c** and **19c** bearing fluorine substituent at the 4-position, showed slight increase in the activity suggesting that the substitution in the 4-position may be tolerated and also suggesting that the halogens incorporation may be advantageous. The introduction of a methoxy group (electron-donating group) at the 4-position of compounds **14b** and **19b** resulted in a partial loss of the activity. In contrast, introduction of chlorine atom (more bulky than fluorine) at the 4- and 3-positions (**14e**, **14f**, **19e** and **19f**) has caused a remarkable enhancement in the antitumor activity against almost all tested tumor cell types. Interestingly, moving the chlorine from the 4- and 3-positions to the 2-position has sharply decreased the antitumor activity with an exception for the impact of **19d** on hepatocellular carcinoma which has resulted in the remarkable IC_{50} value in this study (1.2 μM). Notably, the HT-29 cancer cells were only highly sensitive to the 3- and 4-chloro substituents **14e**, **14f**, **19e** and **19f** which were 2.5-, 1.9-, 2- and 2.6-fold more active than doxorubicin.

The order of anticancer activities of the halogenated derivatives (**14c**–**f** and **19c**–**f**) has widely varied in accordance to the type of the cell line and the aryl group at position 4 of the phthalazine scaffold. Concerning the effect of the halogenated members in the first series, the activities were decreased in the order of 3-Cl > 4-Cl > 4-F > 2-Cl for the HepG2 and HT-29 cancer cells and in the order of 4-Cl > 2-Cl > 4-F > 3-Cl for the MCF-7. For the second series, the activities were decreased in the order of 2-Cl > 3-Cl > 4-F > 4-Cl for HepG2 cancer cells, 4-Cl > 3-Cl > 2-Cl > 4-F for HT-29 and in the order of 3-Cl > 4-Cl > 4-F > 2-Cl for MCF-7 cancer cells. Replacing Cl with the CF_3 at the 3-position has enhanced the activity against the breast cancer as; **19g** ($IC_{50} = 3.85 \pm 0.96$ μM) that has represented the most active derivative against breast cancer cell line MCF-7.

Finally, we can deduce that the substitution pattern on the anilino moiety is a crucial element for the antitumor activity. The incorporation of electron donating groups as the methoxy group is not favorable for the activity. While substitution with bulky electron withdrawing groups as the chlorine or trifluoromethyl groups, has greatly enhanced the activity.

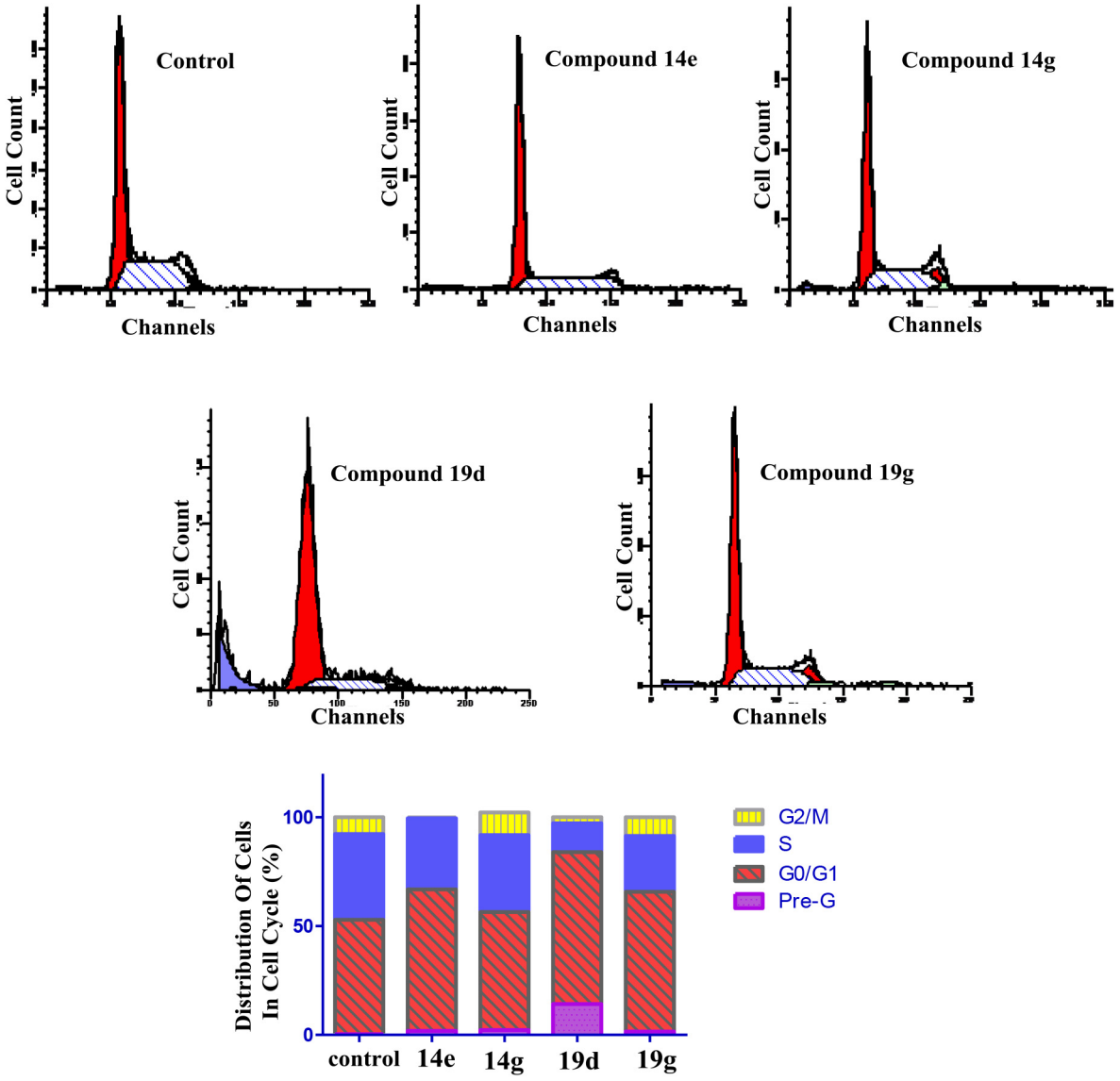

Fig. 2. DNA-flow cytometry analysis for HepG2 cells treated with compounds **14e**, **14g**, **19d** and **19g** for 24 h at their IC_{50} concentrations. The experiments were done in triplicate. Data are mean ± SEM.

2.2.3. Cell-cycle analysis and apoptotic changes

Liver cancer in men is the fifth most frequently diagnosed cancer worldwide but the second most frequent cause of cancer death. In women, it is the seventh most commonly diagnosed cancer and the sixth leading cause of cancer death. An estimated 748,300 new liver cancer cases and 695,900 cancer deaths occurred worldwide in 2008 [33]. Among primary liver cancers, hepatocellular carcinoma (HCC) represents the major histological subtype, accounting for 70%–85% of the total liver cancer burden worldwide [34]. Of activity against HepG2 cancer cells, compounds **14e**, **14g**, **19d** and **19g** were found to be the most active agents. Subsequently, we decided to scrutinize the potential apoptotic effects of these promising agents.

Cell reproduction entails replication of the DNA followed by division of the nucleus and partitioning of the cytoplasm to yield two daughter cells. This sequential routine is known as the 'cell cycle' which comprises four distinct phases. G1 phase is a gap incorporated between nuclear division (M phase) and DNA synthesis (S phase); another gap called G2 phase occurs between S and M. These gaps allow for the repair of DNA damage and replication errors [35]. The effects of compounds **14e**, **14g**, **19d** and **19g** after 24 h of treatment on cell cycle progression were examined in HepG2 cells (Fig. 2). Flow cytometry DNA analysis using propidium iodide for **14e** and **14g** did not induce any significant alterations in the cell-cycle phases of HepG2 cells when compared to control. Interestingly, exposure of HepG2 cells to **19d** induced a significant increase in the percentage of cells at pre-G1 by 28-folds, with concurrent significant reduction in the percentage of cells at G0/G1 and S phases by 2- and 1.9-folds compared to control, respectively. Moreover, treatment with **19g** caused a significant increase in pre-G1 phase percent by 9.4-folds and in S phase percent by 27.7% compared to control, with a concomitant significant decrease in the percentage of cells at G0/G1 phases by 32.3% compared to control.

2.2.4. Annexin V–FITC apoptosis assay

Further evaluation of the apoptotic effect of compounds **14e**, **14g**, **19d** and **19g** was carried out using Annexin V–FITC/PI (AV/PI) dual staining assay (Fig. 3). Flow cytometric analysis revealed that HepG2 cells treated with compounds **14e**, **14g**, **19d** and **19g** showed a significant increase in the percent of annexin V–FITC-positive apoptotic cells (UR + LR) by 2.4-, 2.1-, 9.5- and 2.7-folds compared to control, respectively.

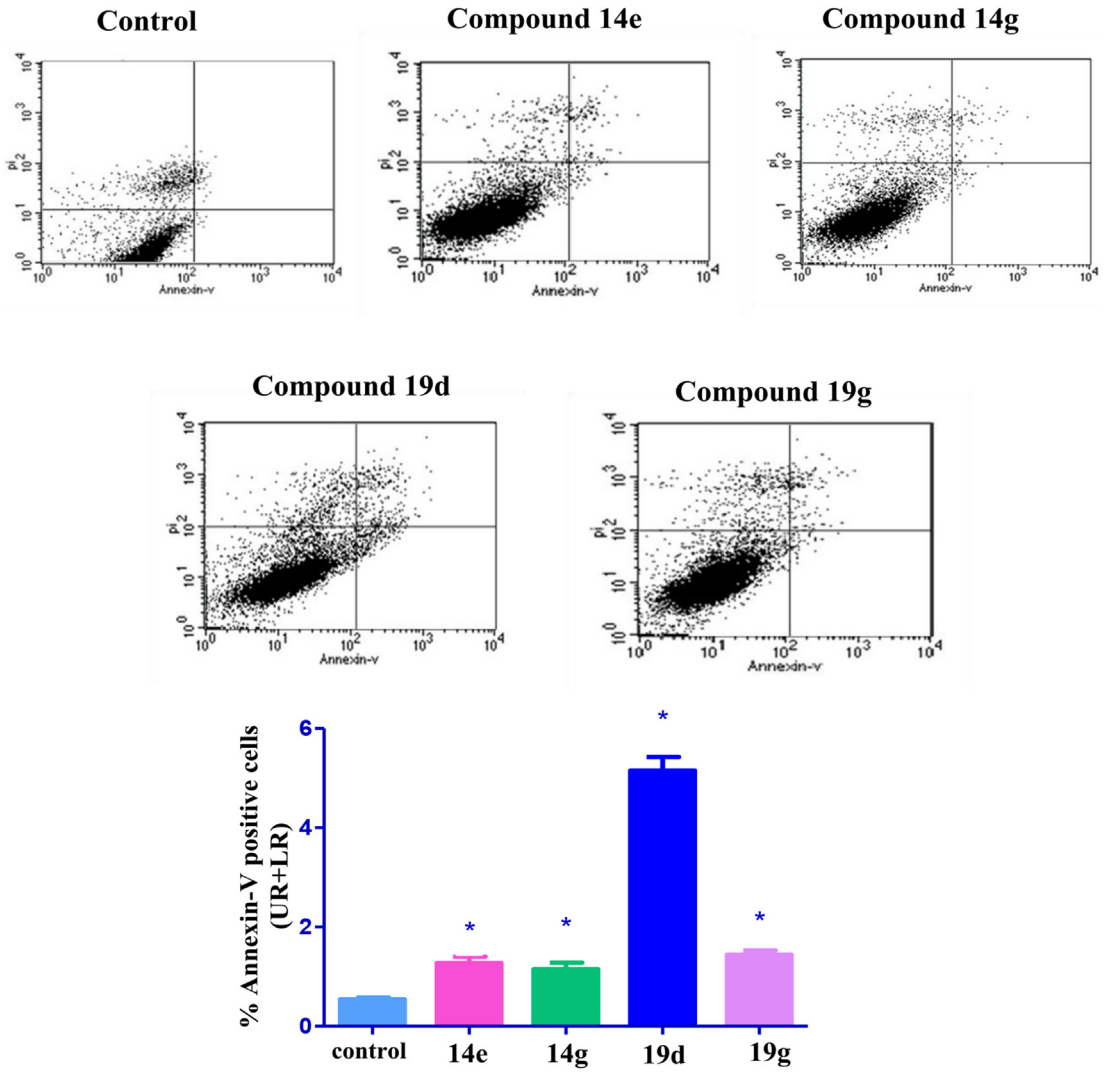

Fig. 3. Effect of compounds **14e**, **14g**, **19d** and **19g** on the percentage of annexin V–FITC-positive staining in HepG2 cells. The experiments were done in triplicates. The four quadrants identified as: LL, viable; LR, early apoptotic; UR, late apoptotic; UL, necrotic. *Significantly different from control at $p < 0.05$.

2.2.5. Effects on mitochondrial apoptosis pathway proteins Bcl-2 and Bax

HepG2 cells treated with **14e**, **14g**, **19d** and **19g** have exhibited significant down-regulation of Bcl-2 by approximately 22, 9.6, 34 and 22%, respectively, compared to the control (Table 2, Fig. 4). Bcl-2 family proteins are an important factor for apoptosis resistance in HCC. Bcl-2 is specifically considered as an important anti-apoptotic protein [36]. Treatment of HepG2 cells with compounds **14e**, **14g**, **19d** and **19g** has resulted in a significant up-regulation of the pro-apoptotic protein Bax by approximately 43.5, 44, 80.2 and 39.9%, respectively, compared to the control (Table 2, Fig. 2). Accordingly, the Bax/Bcl2 ratio showed high values in **14e**, **14g**, **19d** and **19g**. Bax is another member of the Bcl-2 family but has pro-apoptotic effects. Increased expression of Bax is known to be associated with a lack of development of resistance to chemotherapy in many types of cancers including liver cancer [37].

2.2.6. Effects on the level of active caspase-3 (key executor of apoptosis)

Down-regulation of Bcl-2 results in increased levels of free BAX, which in turn leads to activation of the caspase cascade leading to apoptosis [38]. So, the elevated Bax/Bcl2 ratio for compounds **14e**, **14g**, **19d** and **19g** directed us to assess the levels of active caspase-3, a cysteine protease, which is a key executor of apoptosis.

Treatment of HepG2 cells with compounds **14e**, **14g**, **19d** and **19g** significantly increased the level of active caspase-3 by approximately 3-, 2.5-, 4- and 2.8-fold, respectively, compared to the control (Table 2, Fig. 4). The simultaneous up-regulation of the downstream Caspase 3; The hallmark key player in the intrinsic apoptotic pathway, strongly suggests that a cascade of apoptotic markers has been activated as a consequence of Bax/Bcl2 elevation, that eventually led to apoptosis.

Comparing the highly expressed levels of apoptotic markers for the four compounds, as well as the Bax/Bcl2 ratio, it is obvious that the magnitude of the Bax/Bcl2 ratio elevation is proportional to the magnitude of Caspase 3 up-regulation; such that **19d** which is shown to have the highest Bax/Bcl2 ratio, has also the highest levels of Caspase 3 expressed, followed by **14e** and **19g** that show intermediate elevated values of Bax/Bcl2 ratio with corresponding intermediate upregulated levels of Caspase 3. **14g**, which shows the lowest elevation of Bax/Bcl2 ratio, correspondingly exhibits the lowest upregulation of Caspase 3. This suggests a strong correlation between the increased Bax/Bcl2 ratio and the well-known downstream Caspase 3, as key players in the mechanism by which **14e**, **14g**, **19d** and **19g** exert their anticancer effect. Moreover, exposure of HT-29 cells to **14e**, **14g**, **19d** and **19g** showed a significant increase in the protein level of active caspase-3 by 5.6-, 4.3-, 4.8- and 7.1-folds compared to control, respectively (Table 3, Fig. 5).

In conclusion, the enhanced expression of the pro-apoptotic protein Bax and the reduced expression of the anti-apoptotic protein Bcl-2 in addition to boosting caspase-3 levels with a synchronized increase in the Bax/Bcl2 ratio, suggested that **14e**, **14g**, **19d** and **19g** have exhibited their cytotoxic activity through acting as an apoptotic stimuli, at least in part, *via* inducing the intrinsic apoptotic mitochondrial pathway.

Table 2
Effect of compounds **14e**, **14g**, **19d** and **19g** on the level of active caspase-3 and the expression levels of Bcl-2 and Bax in HepG2 cancer cells treated with the compounds at their IC_{50} concentrations.

Compound	Bcl-2 mg/mg protein	Bax ng/mg protein	Caspase-3 nmol/mg protein
Control	10.660 ± 0.024	5.031 ± 0.016	1.774 ± 0.054
14e	8.323 ± 0.037	7.218 ± 0.070	5.585 ± 0.197
14g	9.632 ± 0.045	7.251 ± 0.099	4.492 ± 0.121
19d	6.997 ± 0.031	9.068 ± 0.139	7.096 ± 0.101
19g	8.308 ± 0.093	7.038 ± 0.109	4.945 ± 0.097

Values are the mean ± S.D. of three separate experiments.

3. Conclusion

In summary, we have designed and synthesized fourteen *N*-substitutedphthalazin-1-one derivatives based on the 4-phenyl/benzylphthalazin-1-one scaffold and evaluated their cytotoxic activities against three cancer cell lines (HepG2, HT-29 and MCF-7). Most of the prepared compounds displayed relatively potent and selective cytotoxic activity against HepG2 cancer cell line. In particular, compounds **14e**, **14g** and **19d** displayed the highest activity against HepG2, with IC_{50} values ranging from 1.20 ± 0.09 to 3.50 ± 0.846 μM, and they were able to induce apoptosis in HepG2 cells, as evidenced by reduced expression of the anti-apoptotic protein Bcl-2 and enhanced expression of the pro-apoptotic protein Bax, besides increased caspase-3 levels. These results suggest that compounds **14e**, **14g** and **19d** exert a cytotoxic effect in HepG2 human hepatocellular carcinoma cells, at least in part, *via* activation of the mitochondrial apoptotic pathway. Furthermore, the prepared compounds showed moderate to fair cytotoxicity against HT-29 and MCF-7 cancer cell lines.

From the structure activity relationships (SARs) we can deduce that the replacement of the 4-phenyl group by the benzyl one was unimportant for the cytotoxic activity against HepG2 liver cancer and HT-29 colon cancer, cell lines. While it was essential for the cytotoxicity against MCF-7 breast cancer cell line. The introduction of a halogen atom on the anilino moiety plays an important role in enhancing the antitumor activities in a widely varied order according to the type of the cell line and the aryl group at the 4-position of the phthalazine scaffold. Further studies are in progress in our laboratories and will be reported upon in the future.

4. Experimental

4.1. Chemistry

4.1.1. General

Melting points were measured with a Stuart melting point apparatus and were uncorrected. IR spectra (KBr disks) were recorded with a Pye Unicam SP 1000 IR spectrophotometer. The NMR spectra were recorded by Varian Gemini-300BB 300 MHz FT-NMR spectrometers (Varian Inc., Palo Alto, CA). ^1H and ^{13}C spectra were run at 300 and 75 MHz, respectively, in deuterated dimethylsulphoxide (DMSO-d_6). Chemical shifts (δ_H) are reported relative to TMS as internal standard. All coupling constant (J) values are given in hertz. Chemical shifts (δ_C) are reported relative to DMSO-d_6 as internal standards. The abbreviations used are as follows: s, singlet; d, doublet; m, multiplet. Mass spectra were recorded on Helwett Packard 5988 spectrometer at 70 eV. Reaction courses and product mixtures were routinely monitored by thin layer chromatography (TLC) on silica gel precoated F_{254} Merck plates. Unless otherwise noted, all solvents and reagents were commercially available and used without further purification.

4.1.2. 2-Chloro-N-(unsubstituted/substitutedphenyl)acetamides ***11a–g***

Compounds **11a–g** were prepared according to the literatures procedures [39–41].

4.1.3. 4-Phenyl-1(2H)-phthalazinone (***13***)

Compound **13** was prepared according to the literature procedure [42]. A solution of hydrazine sulfate (4.0 g, 30.4 mmol) and sodium hydroxide (2.4 g, 60.8 mmol) in 20 mL of water was heated on a steam bath for 20 min. The hot solution was added to a hot

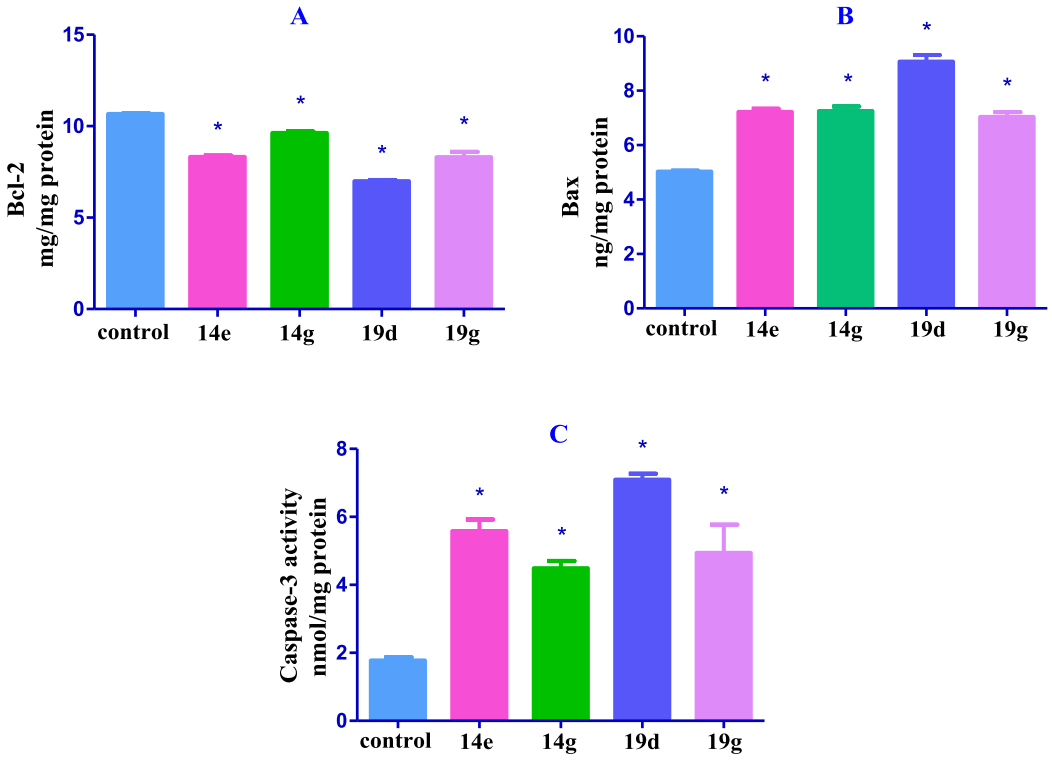

Fig. 4. Effect of compounds **14e**, **14g**, **19d** and **19g** on the protein levels of A) Bcl-2; B) Bax and C) active caspase-3 in HePG2 cells treated with the compounds at their IC_{50} concentrations. Data are mean ± SEM. *Significantly different from control at $p < 0.05$.

aqueous solution of 2-benzoylbenzoic acid (**12**) (6.9 g, 30.4 mmol). The reaction mixture was heated under reflux for 1 h. After cooling and addition of hydrochloric acid, the residue obtained was filtered, washed with water and crystallized from 2-propanol to give 4-phenyl-1(*2H*)-phthalazinone (**13**), m.p. 239–241 °C. ^{1}H NMR (DMSO-d_6) δ ppm: 7.53–7.61 (m, 5H, Ar–H), 7.66–7.70 (m, 1H, H-5 phthalazine), 7.86–7.93 (m, 2H, H-6 and H-7 phthalazine), 8.32–8.35 (m, 1H, H-8 phthalazine), 12.84 (s, 1H, D_2O exchangeable, NH).

4.1.4. General procedure for preparation of target compounds ***14a–g***

To a stirred mixture of 4-phenyl-1(2*H*)-phthalazinone (**13**) (0.45 g, 2 mmol), anhydrous potassium carbonate (0.55 g, 0.004 mol) and catalytic amount of KI in dry acetone, a solution of the appropriate 2-chloro-*N*-(unsubstituted/substitutedphenyl) acetamide **11a–g** (2 mmol) in dry acetone was added. The mixture was heated under reflux for 11 h, then filtered while hot and the precipitate was washed with water several times. The solid product was collected and crystallized from an ethanol/dioxan mixture (5:1) to give compounds **14a–g**.

Table 3
Effect of compounds **14e**, **14f**, **19e** and **19f** on the level of active caspase-3 in HT-29 cancer cells treated with the compounds at their IC_{50} concentrations.

Compound	Caspase-3 nmol/mg protein
Control	0.581 ± 0.013
14e	3.254 ± 0.095
14f	2.508 ± 0.107
19e	2.795 ± 0.079
19f	4.142 ± 0.163

Values are the mean ± S.D. of three separate experiments.

*4.1.4.1. 2-(1-Oxo-4-phenylphthalazin-2(1H)-yl)-N-phenylacetamide (**14a**).* White crystals (yield 69%), m.p. 268–269 °C; IR (KBr, ν cm^{-1}): 3264 (NH), 1664 (C=O) and 1542 (C=N); ^{1}H NMR (DMSO-d_6) δ ppm: 5.03 (s, 2H, $COCH_2$), 7.03 (t, 1H, J = 8.7 Hz, H-4 of NH–C_6H_5), 7.28–7.34 (m, 2H, H-3 and H-5 of NH–C_6H_5), 7.55–7.63

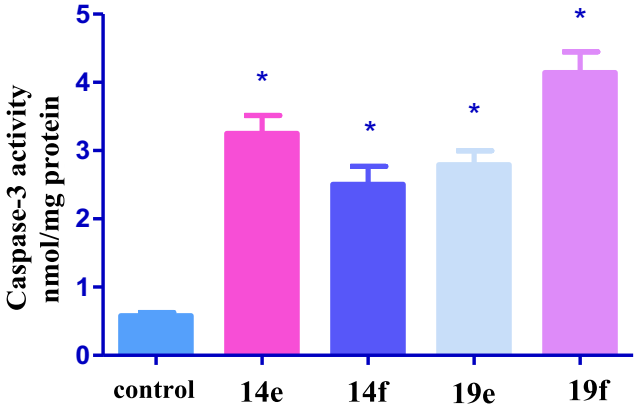

Fig. 5. Effect of compounds **14e**, **14f**, **19e** and **19f** on the protein level of active caspase-3 in HT-29 cells treated with the compounds at their IC_{50} concentrations. Data are mean ± SEM. *Significantly different from control at $p < 0.05$.

(m, 7H, H-2, H-6 of NH–C_6H_5 and 5H of Ar–H), 7.72–7.77 (m, 1H, H-5 phthalazine), 7.91–7.96 (m, 2H, H-6 and H-7 phthalazine), 8.36–8.40 (m, 1H, H-8 phthalazine), 10.04 (s, 1H, D_2O exchangeable, NH); ^{13}C NMR (DMSO-d_6) δ ppm: 54.22 (–CH_2CO), 119.17, 123.41, 126.44, 126.63, 127.39, 128.56, 128.74, 129.14, 129.35, 131.95, 133.68, 134.52, 138.67, 146.17, 154.24, 158.36, 162.90, 165.47 (C=O); MS *m/z* [%]: 263 [46.18], 235 [100].

*4.1.4.2. N-(4-methoxyphenyl)-2-(1-oxo-4-phenylphthalazin-2(1H)-yl)acetamide (**14b**).* White crystals (yield 65%), m.p. 273–275 °C; IR (KBr, ν cm^{-1}): 3270 (NH), 1666 (C=O) and 1540 (C=N); ^{1}H NMR (DMSO-d_6) δ ppm: 3.72 (s, 3H, OCH_3), 5.00 (s, 2H, $COCH_2$), 6.87 (d, 2H, J = 8.7 Hz, H-3 and H-5 of 4-$OCH_3C_6H_4$), 7.47 (d, 2H, J = 9.3 Hz, H-2 and H-6 of 4-$OCH_3C_6H_4$), 7.55–7.63 (m, 5H, Ar–H), 7.71–7.76 (m, 1H, H-5 phthalazine), 7.90–7.94 (m, 2H, H-6 and H-7 phthalazine), 8.37–8.40 (m, 1H, H-8 phthalazine), 10.04 (s, 1H, D_2O exchangeable, NH); ^{13}C NMR (DMSO-d_6) δ ppm: 54.35 (–CH_2CO), 55.11 (O–CH_3), 113.87, 120.57, 126.44, 126.60, 127.42, 128.55, 128.73, 129.12, 129.34, 131.80, 131.91, 133.64, 134.54, 146.14, 155.32, 158.37, 164.99 (C=O); MS *m/z* [%]: 385 [6.78], 262 [47.84], 122 [100].

*4.1.4.3. N-(4-fluorophenyl)-2-(1-oxo-4-phenylphthalazin-2(1H)-yl) acetamide (**14c**).* White crystals (yield 73%), m.p. 260–262 °C; IR (KBr, ν cm^{-1}): 3246 (NH), 1660 (C=O) and 1539 (C=N); ^{1}H NMR (DMSO-d_6) δ ppm: 5.02 (s, 2H, $COCH_2$), 7.12 (d, 2H, J = 8.7 Hz, H-3 and H-5 of 4-FC_6H_4), 7.55–7.63 (m, 7H, H-2, H-6 of 4-FC_6H_4 and 5H of Ar–H), 7.72–7.75 (m, 1H, H-5 phthalazine), 7.92–7.95 (m, 2H, H-6 and H-7 phthalazine), 8.37–8.40 (m, 1H, H-8 phthalazine), 10.32 (s, 1H, D_2O exchangeable, NH); ^{13}C NMR (DMSO-d_6) δ ppm: 54.30 (–CH_2CO), 115.17, 120.92, 126.44, 127.39, 128.56, 128.73, 129.14, 129.34, 130.33, 131.95, 133.68, 134.51, 135.06, 146.20, 156.47, 158.36, 159.65, 165.44 (C=O); MS *m/z* [%]: 273 [13.59], 278 [31.48], 110 [100].

*4.1.4.4. N-(2-chlorophenyl)-2-(1-oxo-4-phenylphthalazin-2(1H)-yl) acetamide (**14d**).* White crystals (yield 63%), m.p. 212–213 °C; IR (KBr, ν cm^{-1}): 32,922 (NH), 1668 (C=O) and 1587 (C=N); (DMSO-d_6) δ ppm: 5.11 (s, 2H, $COCH_2$), 7.19 (t, 1H, J = 7.8 Hz, H-4 of 2-ClC_6H_4), 7.31 (t, 1H, J = 7.8 Hz, H-5 of 2-ClC_6H_4), 7.49 (d, 1H, J = 7.8 Hz, H-3 of 2-ClC_6H_4), 7.56–7.64 (m, 5H, Ar–H), 7.71–7.74 (m, 2H, H-6 of 2-ClC_6H_4 and H-5 phthalazine), 7.90–7.95 (m, 2H, H-6 and H-7 phthalazine), 8.37–8.41 (m, 1H, H-8 phthalazine), 9.89 (s, 1H, D_2O exchangeable, NH); ^{13}C NMR (DMSO-d_6) δ ppm: 54.07 (–CH_2CO), 125.85, 126.39, 126.64, 127.41, 128.55, 128.72, 129.14, 129.36, 129.49, 131.95, 133.67, 134.49, 134.52, 146.31, 158.37, 166.09 (C=O); MS *m/z* [%]: 389 [1.37], 262 [8.15], 51 [100].

*4.1.4.5. N-(3-chlorophenyl)-2-(1-oxo-4-phenylphthalazin-2(1H)-yl) acetamide (**14e**).* White crystals (yield 77%), m.p. 231–233 °C; IR (KBr, ν cm^{-1}): 3261 (NH), 1663 (C=O) and 1585 (C=N); ^{1}H NMR (DMSO-d_6) δ ppm: 5.04 (s, 2H, $COCH_2$), 7.12 (d, 1H, J = 6.9 Hz, H-4 of 3-ClC_6H_4), 7.32 (t, 1H, J = 8.4 Hz, H-5 of 3-ClC_6H_4), 7.44 (d, 1H, J = 8.4 Hz, H-6 of 3-ClC_6H_4), 7.56–7.63 (m, 5H, Ar–H), 7.72–7.75 (m, 1H, H-5 phthalazine), 7.79 (s, 1H, H-2 of 3-ClC_6H_4), 7.91–7.98 (m, 2H, H-6 and H-7 phthalazine), 8.36–8.40 (m, 1H, H-8 phthalazine), 10.51 (s, 1H, D_2O exchangeable, NH); MS *m/z* [%]: 389 [2.62], 277 [7.86], 234 [69.16].

*4.1.4.6. N-(4-chlorophenyl)-2-(1-oxo-4-phenylphthalazin-2(1H)-yl) acetamide (**14f**).* White crystals (yield 79%), m.p. 253–254 °C; IR (KBr, ν cm^{-1}): 3249 (NH), 1659 (C=O) and 1527 (C=N); ^{1}H NMR (DMSO-d_6) δ ppm: 5.03 (s, 2H, $COCH_2$), 7.34 (d, 2H, J = 8.7 Hz, H-3 and H-5 of 4-ClC_6H_4), 7.55–7.63 (m, 7H, H-2, H-6 of 4-ClC_6H_4 and 5H of Ar–H), 7.71–7.76 (m, 1H, H-5 phthalazine), 7.90–7.97 (m, 2H, H-6 and H-7 phthalazine), 8.37–8.40 (m, 1H, H-8 phthalazine), 10.46 (s, 1H, D_2O exchangeable, NH); ^{13}C NMR (DMSO-d_6) δ ppm: 54.40 (–CH_2CO), 120.72, 126.45, 126.66, 127.00, 127.36, 128.57, 128.68, 128.72, 129.15, 129.35, 131.99, 133.72, 134.49, 137.62, 146.22, 158.36, 165.69 (C=O); MS *m/z* [%]: 389 [14.1], 354 [18.69], 221 [13.11].

*4.1.4.7. 2-(1-Oxo-4-phenylphthalazin-2(1H)-yl)-N-(3-(trifluoromethyl)phenyl)acetamide (**14g**).* White crystals (yield74%), m.p. 192–193 °C; IR (KBr, ν cm^{-1}): 3267 (NH), 1626 (CO) and 1574 (C=N); ^{1}H NMR (DMSO-d_6) δ ppm: 5.07 (s, 2H, $COCH_2$), 7.41 (d, 1H, J = 7.5 Hz, H-4 of 3-C $F_3C_6H_4$), 7.54–7.62 (m, 6H, H-5 of 3-C $F_3C_6H_4$ and 5H of Ar–H), 7.62–7.77 (m, 2H, H-6 of 3-$CF_3C_6H_4$ and H-5 phthalazine), 7.91–7.98 (m, 2H, H-6 and H-7 phthalazine), 8.09 (s, 1H, H-2 of 3-$CF_3C_6H_4$), 8.37–8.40 (m, 1H, H-8 phthalazine), 10.66 (s, 1H, D_2O exchangeable, NH); ^{13}C NMR (DMSO-d_6) δ ppm: 54.46 (–CH_2CO), 115.28, 119.83, 122.73, 126.44, 126.66, 127.34, 128.56, 128.73, 129.15, 129.34, 130.04, 132.00, 133.73, 134.47, 139.38, 146.32, 158.40, 166.19 (C=O); MS *m/z* [%]: 424 [1.38], 423 [1.38], 381 [100].

*4.1.5. 3-Benzalphthalide (**17**)*

Following a procedure adopted by Weiss [43], phthalic anhydride (**15**) (10.0 g, 67.5 mmol) was condensed with phenylacetic acid (**16**) (11.0 g, 81 mmol) in the presence of freshly fused sodium acetate (0.26 g) in a Dean–Stark apparatus for 4 h at 240 °C. After cooling to room temperature, the solid reaction mixture was crystallized from ethanol to give 3-benzalphthalide (**17**): m.p. 100–102 °C.

*4.1.6. 4-Benzylphthalazin-1(2H)-one (**18**)*

A mixture of compound **17** (11.1 g, 0.05 mol) and hydrazine sulfate (7.8 g, 0.06 mol) was treated with NaOH solution (2 M, 50 mL), water (60 mL) and ethanol (15 mL) and the mixture was heated to 95 °C for 15 h and then allowed to cool to room temperature. The reaction mixture was diluted with water (500 mL) and the solid was collected by filtration, washed with water, dried *in vacuo* to give compound **18** [44], m.p. 200–202 °C. ^{1}H NMR (DMSO-d_6) δ ppm: 7.15–7.32 (m, 5H, Ar–H), 7.73–7.86 (m, 2H, H-6 and H-7 phthalazine), 7.90 (d, 1H, J = 7.8 Hz, H-5 phthalazine), 8.24 (d, 1H, J = 7.5 Hz, H-8 phthalazine), 12.57 (s, 1H, D_2O exchangeable, NH).

*4.1.7. General procedure for preparation of target compounds **19a–g***

To a stirred mixture of 4-benzylphthalazin-1(*2H*)-one (**18**) (0.57 g, 2 mmol), anhydrous potassium carbonate (0.55 g, 4 mmol) and catalytic amount of KI in dry acetone, a solution of the appropriate 2-chloro-*N*-(substitutedphenyl) acetamide **11a–g** (2 mmol) in dry acetone was added. The mixture was heated under reflux for 9 h, cooled then poured into water. The solid product was collected, washed with water and crystallized from an EtOH/dioxane.

*4.1.7.1. 2-(4-Benzyl-1-oxophthalazin-2(1H)-yl)-N-phenylacetamide (**19a**).* White crystals (yield 67%), m.p. 235–236 °C; IR (KBr, ν cm^{-1}): 3268 (NH), 1661 (C=O), 1549 (C=N); ^{1}H NMR (DMSO-d_6) δ ppm: 4.33 (s, 2H, CH_2), 5.01 (s, 2H, $COCH_2$), 7.07 (t, 1H, J = 7.2 Hz, H-4 of NH–C_6H_5), 7.16–7.36 (m, 7H, H-3, H-5 of NH–C_6H_5 and 5H of Ar–H), 7.59 (d, 2H, J = 7.8 Hz, H-2 and H-6 of NH–C_6H_5), 7.80–7.89 (m, 2H, H-6 and H-7 phthalazine), 7.92 (d, 1H, J = 7.2 Hz, H-5 phthalazine), 8.28 (d, 1H, J = 6.9 Hz, H-8 phthalazine), 10.29 (s, 1H, D_2O exchangeable, NH); ^{13}C NMR (DMSO-d_6) δ ppm: 37.57 (benzylic CH_2), 54.06 (–CH_2CO), 119.15, 123.36, 125.83, 126.34, 127.49, 128.30, 128.51, 128.76, 128.86, 131.70, 133.40, 138.06, 138.73, 144.99, 158.57, 165.64 (C=O); MS *m/z* [%]: 277 [68.41], 235 [93.94].

*4.1.7.2. 2-(4-Benzyl-1-oxophthalazin-2(1H)-yl)-N-(4-methoxyphenyl)acetamide (**19b**).* White crystals (yield67%), m.p. 236–237 °C; IR (KBr, ν cm^{-1}): 3270 (NH), 1665 (C=O), 1537 (C=N); (DMSO-d_6) δ ppm: 3.72 (s, 3H, OCH_3), 4.33 (s, 2H, CH_2), 4.96 (s, 2H, $COCH_2$), 6.88 (d, 2H, H-3 and H-5 f 4-$OCH_3C_6H_4$ J = 8.7 Hz), 7.16–7.36 (m, 5H, Ar–H), 7.48 (d, 2H, J = 8.7 Hz, H-2 and H-6 of 4-$OCH_3C_6H_4$), 7.80–7.89 (m, 2H, H-6 and H-7 phthalazine), 7.92 (d, 1H, J = 7.2 Hz, H-5 phthalazine), 8.28 (d, 1H, J = 6.9 Hz, H-8 phthalazine), 10.12 (s, 1H, D_2O exchangeable, NH). MS m/z [%]: 399 [2.85], 277 [48.87].

*4.1.7.3. 2-(4-Benzyl-1-oxophthalazin-2(1H)-yl)-N-(4-fluorophenyl) acetamide (**19c**).* White crystals (yield 67%), m.p. 202–203 °C; IR (KBr, ν cm^{-1}): 3276 (NH), 1656 (C=O), 1533 (C=N); ^{1}H NMR (DMSO-d_6) δ ppm: 4.33 (s, 2H, CH_2), 4.99 (s, 2H, $COCH_2$), 7.13–7.21 (m, 2H, H-3 and H-5 of 4-FC_6H_4), 7.25–7.36 (m, 5H, Ar–H), 7.59–7.64 (m, 2H, H-2 and H-6 of 4-FC_6H_4), 7.80–7.09 (m, 2H, H-6 and H-7 phthalazine), 7.92 (d, 1H, J = 7.5 Hz, H-5 phthalazine), 8.27 (d, 1H, J = 7.5 Hz, H-8 phthalazine), 10.35 (s, 1H, D_2O exchangeable, NH). MS m/z [%]: 388 [0.15], 387 [1.04], 277 [73.46].

*4.1.7.4. 2-(4-Benzyl-1-oxophthalazin-2(1H)-yl)-N-(2-chlorophenyl) acetamide (**19d**).* White crystals (yield 67%), m.p. 185–187 °C; IR (KBr, ν cm^{-1}): 3364 (NH), 1653 (C=O), 1528 (C=N); ^{1}H NMR (DMSO-d_6) δ ppm: 4.33 (s, 2H, CH_2), 5.08 (s, 2H, $COCH_2$), 7.18–7.36 (m, 7H, H-4, H-5 of 2-ClC_6H_4 and H of Ar–H), 7.49 (d, 1H, J = 8.4 Hz, H-3 of 2-ClC_6H_4), 7.74 (d, 1H, J = 8.4 Hz, H-6 of 2-ClC_6H_4), 7.82–7.89 (m, 2H, H-6 and H-7 phthalazine), 7.92 (d, 1H, J = 7.2 Hz, H-5 phthalazine), 8.28 (d, 1H, J = 7.2 Hz, H-8 phthalazine), 9.81 (s, 1H, D_2O exchangeable, NH). ^{13}C NMR (DMSO-d_6) δ ppm: 37.58 (benzylic $\underline{C}H_2$), 53.77 (–$\underline{C}H_2CO$), 125.83, 126.36, 126.46, 127.43, 127.49, 128.32, 128.49, 128.85, 129.51, 131.72, 133.41, 134.52, 138.03, 145.12, 158.59, 166.22 ($\underline{C}$=O); MS m/z [%]: 405 [0.53], 403 [1.7], 277 [81.95].

*4.1.7.5. 2-(4-Benzyl-1-oxophthalazin-2(1H)-yl)-N-(3-chlorophenyl) acetamide (**19e**).* White crystals (yield67%), m.p. 163–164 °C; IR (KBr, ν cm^{-1}): 3279 (NH), 1683 (C=O), 1562 (C=N); ^{1}H NMR (DMSO-d_6) δ ppm: 4.33 (s, 2H, CH_2), 5.03 (s, 2H, $COCH_2$), 7.16–7.36 (m, 5H, Ar–H), 7.41 (d, 1H, H-4 of 3-ClC_6H_4 J = 7.8 Hz), 7.55 (t, 1H, H-5 of 3-ClC_6H_4 J = 7.8 Hz), 7.77–7.90 (m, 2H, H-6 and H-7 phthalazine), 7.91 (d, 1H, H-5 phthalazine J = 7.5 Hz), 8.09 (s, 1H, H-2 of 3-ClC_6H_4), 8.27 (d, 1H, H-8 phthalazine J = 6.9 Hz), 10.66 (s, 1H, D_2O exchangeable, NH); ^{13}C NMR (DMSO-d_6) δ ppm: 37.55 (benzylic $\underline{C}H_2$), 54.20 (–$\underline{C}H_2CO$), 115.24, 119.74, 122.22, 122.74, 125.86, 126.34, 127.45, 128.30, 128.87, 129.26, 129.68, 130.05, 131.75, 133.45, 138.03, 139.53, 145.15, 158.60, 166.36 ($\underline{C}$=O); MS m/z [%]: 403 [5.69], 277 [100].

*4.1.7.6. 2-(4-Benzyl-1-oxophthalazin-2(1H)-yl)-N-(4-chlorophenyl) acetamide (**19f**).* White crystals (yield 67%), m.p. 224–225 °C; IR (KBr, ν cm^{-1}): 3272 (NH), 1653 (C=O), 1528 (C=N); ^{1}H NMR (DMSO-d_6) δ ppm: 4.33 (s, 2H, CH_2), 5.00 (s, 2H, $COCH_2$), 7.16–7.33 (m, 5H, Ar–H), 7.37 (d, 2H, J = 6.6 Hz, H-3 and H-5 of 4-ClC_6H_4), 7.61 (d, 2H, J = 6.9 Hz, H-2 and H-6 of 4-ClC_6H_4), 7.80–7.90 (m, 2H, H-6 and H-7 phthalazine), 7.92 (d, 1H, J = 7.5, Hz H-5 phthalazine), 8.27 (d, 1H, J = 6.9 Hz, H-8 phthalazine), 10.43 (s, 1H, D_2O exchangeable, NH); ^{13}C NMR (DMSO-d_6) δ ppm: 37.56 (benzylic $\underline{C}H_2$), 54.10 (–$\underline{C}H_2CO$), 120.72, 125.85, 126.34, 126.47, 126.98, 127.46, 128.30, 128.52, 128.68, 128.86, 131.73, 133.43, 137.67, 138.04, 145.06, 158.57, 165.84 ($\underline{C}$=O); MS m/z [%]: 403 [2.92], 277 [78.38], 234 [37.34].

*4.1.7.7. 2-(4-Benzyl-1-oxophthalazin-2(1H)-yl)-N-(3-(trifluoromethyl)phenyl) acetamide (**19g**).* White crystals (yield 67%), m.p. 191–192 °C; IR (KBr, ν cm^{-1}): 3287 (NH), 1665 (C=O) and 1537 (C=N); ^{1}H NMR (DMSO-d_6) δ ppm: 4.33 (s, 2H, CH_2), 5.01 (s, 2H, $COCH_2$), 7.12–7.39 (m, 7H, H-4 and H5 of 3-$CF_3C_6H_4$ and 5H of Ar–H), 7.46 (d, 1H, J = 9.3 Hz, H-6 of 3-$CF_3C_6H_4$), 7.79 (s, 1H, H-2 of 3-$CF_3C_6H_4$), 7.80–7.90 (m, 2H, H-6 and H-7 phthalazine), 7.93 (d, 1H, J = 7.2, Hz H-5 phthalazine), 8.27 (d, 1H, J = 6.9 Hz, H-8 phthalazine), 10.51 (s, 1H, D_2O exchangeable, NH); ^{13}C NMR (DMSO-d_6) δ ppm: 37.57 (benzylic $\underline{C}H_2$), 54.15 (–$\underline{C}H_2CO$), 117.55, 118.68, 123.11, 125.84, 126.35, 126.47, 127.45, 128.30, 128.51, 128.86, 130.50, 131.73, 133.09, 133.43, 138.03, 140.13, 145.11,158.59, 166.12 ($\underline{C}$=O); MS m/z [%]: 389 [14.1], 354 [18.69], 221 [13.11].

4.2. Biological evaluation

4.2.1. In vitro cytotoxic activity

HepG2 liver cancer, HT-29 colon cancer and MCF-7 breast cancer cell lines were obtained from the National Cancer Institute (Cairo, Egypt). HT-29 cells were grown in DMEM while HepG2 and MCF-7 were grown in RPMI-1640. Media were supplemented with 10% heat-inactivated FBS, 50 units/mL of penicillin and 50 g/mL of streptomycin and maintained at 37 °C in a humidified atmosphere containing 5% CO_2. The cells were maintained as a "monolayer culture" by serial subculturing. Cytotoxicity was determined using the SRB method as previously described by Skehan et al. [32]. Exponentially growing cells were collected using 0.25% trypsin-EDTA and seeded in 96-well plates at 1000–2000 cells/well in supplemented DMEM medium. After 24 h, cells were incubated for 72 h with various concentrations of the tested compounds as well as doxorubicin as the reference compound. Following 72 h of treatment, the cells were fixed with 10% trichloroacetic acid for 1 h at 4 °C. Wells were stained for 10 min at room temperature with 0.4% SRB dissolved in 1% acetic acid. The plates were air dried for 24 h, and the dye was solubilized with Tris–HCl for 5 min on a shaker at 1600 rpm. The optical density (OD) of each well was measured spectrophotometrically at 564 nm with an ELISA microplate reader (ChroMate-4300, FL, USA). The IC_{50} values were calculated according to the equation for Boltzmann sigmoidal concentration–response curve using the nonlinear regression models (GraphPad, Prism Version 5). The results reported are means of at least three separate experiments. Significant differences were analyzed by one-way ANOVA wherein the differences were considered to be significant at $P < 0.05$.

4.2.2. Cell culture and lysate collection

Hepatocellular carcinoma human HepG2 cells were cultured in RPMI and colon cancer HT-29 cells were cultured in DMEM + 10% FBS + 5% penicillin/streptomycin and were incubated at humidified 5% CO_2 and maintained at 37 °C. HepG2 cells were treated with the IC_{50} concentration of **14e**, **14g**, **19d** and **19g** (3.29, 3.50, 1.20 and 3.52 μM, respectively), while HT-29 cells were treated with the IC_{50} concentration of **14e**, **14f**, **19e** and **19f** (3.05, 4.02, 3.68 and 2.98 μM, respectively). HepG2 and HT-29 cells were cultured as a monolayer in T-25 flasks and were seeded to attain 30% confluency prior to treatment. The main 100 mM stock dissolved in DMSO was diluted with cell culture medium in order to reach the previously determined IC_{50} concentration of each preparation. After 72 h of treatment, cells were collected *via* trypsinization and centrifuged at 10000 rpm. The pellet was then rinsed with PBS and lysed in RIPA lysis buffer at 4 °C for 45 min, then centrifuged at 14000 rpm for 20 min to remove the cellular debris. Lysates were then collected and stored at −80 °C for later protein determination and immunoassays.

4.2.3. Cell cycle analysis

The HepG2 cells were treated with 3.29, 3.5, 1.2 and 3.52 μM of compounds **14e**, **14g**, **19d** and **19g**, respectively for 24 h. After treatment, the cells were washed twice with ice-cold PBS, collected

by centrifugation, and fixed in ice-cold 70% (v/v) ethanol, washed with PBS, re-suspended with 0.1 mg/ml RNase, stained with 40 mg/ml PI, and analyzed by flow cytometry using FACScalibur (Becton Dickinson). The cell cycle distributions were calculated using CellQuest software (Becton Dickinson).

4.2.4. Annexin V–FITC apoptosis assay

The HepG2 cells were seeded as described above and then incubated with different treatments for 24 h. Cells were harvested, washed twice with PBS and centrifuged. In brief, 10^5 of cells were treated with Annexin V–FITC and propidium iodide (PI) using the apoptosis detection kit (BD Biosciences, San Jose, CA) according to the manufacturer's protocol. Annexin V–FITC and PI binding were analyzed by flow cytometry on FACScalibur (BD Biosciences, San Jose, CA) without gating restrictions using 10,000 cells. Data were collected using logarithmic amplification of both the FL1 (FITC) and the FL2 (PI) channels. Quadrant analysis of co-ordinate dot plots was performed with CellQuest software. Unstained cells were used to adjust the photomultiplier voltage and for compensation setting adjustment to eliminate spectral overlap between the FL1 and the FL2 signals.

4.2.5. ELISA immunoassay

The levels of the apoptotic markers caspase-3 and Bax as well as the anti-apoptotic marker Bcl-2 were assessed using ELISA colorimetric kits per the manufacturer's instructions. The main principle of sandwich ELISA is the quantification of a specific protein through its containment in a sandwich of specific antibodies conjugated to the colorimetric TMB substrate, whose intensity is proportional to the protein quantity and is measured spectrophotometrically.

The cell lysate was diluted 10 times, and 100 μl (50 μg protein) was added to the wells of three separate microtiter plates for the three ELISA kits that were precoated with primary antibodies specific to caspase-3, Bax and Bcl-2, respectively. A secondary biotin-linked antibody specific to the protein captured by the primary antibody was added to bind the captured protein, forming a "sandwich" of specific antibodies around the desired protein in the cell lysate. The streptavidin-HRP complex was then used to bind the biotin-linked secondary antibody through its streptavidin portion. The HRP domain reacted with the added TMB substrate, forming a colored product that was measured at 450 nm by a plate reader (ChroMate-4300, FL, USA) after the reaction was terminated by the addition of stop solution.

4.2.6. Statistical analysis

The data are presented as the mean ± S.D. Comparisons were carried out using one-way analysis of variance followed by Tukey–Kramer's test for post hoc analysis. Statistical significance was considered to be $P < 0.05$. All statistical analyses were performed using GraphPad InStat software, version 3.05 (GraphPad Software, La Jolla, CA). Graphs were plotted using GraphPad Prism software, version 5.00 (GraphPad Software, La Jolla, CA).

Acknowledgments

The authors would like to extend their sincere appreciation to the Deanship of Scientific Research at King Saud University for its funding of this research through the Research Group Project no. RGP-VPP-321. Department of Pharmaceutical Chemistry, Faculty of Pharmacy, Egyptian Russian University, Cairo, Egypt, is highly appreciated for supporting this research.

Appendix A. Supplementary data

Supplementary data related to this article can be found online at http://dx.doi.org/10.1016/j.ejmech.2014.10.064.

References

[1] C. Avendano, J.C. Menéndez, Medicinal Chemistry of Anticancer Drugs, First ed., Elsevier, 2008, p. 1 (Chapter 1).
[2] K. Nepali, S. Sharma, M. Sharma, P.M.S. Bedi, K.L. Dhar, Eur. J. Med. Chem. 77 (2014) 422–487.
[3] I.H. Hall, B.J. Barnes, E.S. Ward, J.R. Wheaton, K.A. Shaffer, S.E. Cho, A.E. Warren, Arch. Pharm. Pharm. Med. Chem. 334 (2001) 229–234.
[4] I.H. Hall, E.S. Hall, O.T. Wong, Anti Cancer Drugs 3 (1992) 55–62.
[5] I.H. Hall, D.W. Covington, J.R. Wheaton, R.A. Izydore, X. Zhou, Pharmazie 56 (2001) 168–174.
[6] M.C. Cardia, S. Distinto, E. Maccioni, A. Plumitallo, L. Sanna, M.L. Sanna, S. Vigo, J. Heterocycl. Chem. 46 (2009) 674–679.
[7] S.L. Zhang, Y.J. Liu, Y.F. Zhao, Q.T. Guo, P. Gong, Chin. Chem. Lett. 21 (2010) 1071–1074.
[8] S. Zhang, Y. Zhao, Y. Liu, D. Chen, W. Lan, Q. Zhao, C. Dong, L. Xia, P. Gong, Eur. J. Med. Chem. 45 (2010) 3504–3510.
[9] Y. Liu, S. Zhang, Y. Li, J. Wang, Y. Song, P. Gong, Arch. Pharm. Chem. Life Sci. 345 (2012) 287–293.
[10] J. Li, Y.F. Zhao, X.Y. Yuan, J.X. Xu, P. Gong, Molecules 11 (2006) 574–582.
[11] X. Zhai, J. Li, L. He, S. Zheng, Y.B. Zhang, P. Gong, Chin. Chem. Lett. 19 (2008) 29–32.
[12] K. Miller-Moslin, S. Peukert, R.K. Jain, M.A. McEwan, R. Karki, L. Llamas, N. Yusuff, F. He, Y. Li, Y. Sun, M. Dai, L. Perez, W. Michael, T. Sheng, H. Lei, R. Zhang, J. Williams, A. Bourret, A. Ramamurthy, J. Yuan, R. Guo, M. Matsumoto, A. Vattay, W. Maniara, A. Amaral, M. Dorsch, J.F. Kelleher, J. Med. Chem. 52 (2009) 3954–3968.
[13] B.S. Lucas, W. Aaron, S. An, R.J. Austin, M. Brown, H. Chan, A. Chong, R. Hungate, T. Huang, B. Jiang, M.G. Johnson, J.A. Kaizerman, G. Lee, D.L. McMinn, J. Orf, J.P. Powers, M. Rong, M.M. Toteva, C. Uyeda, D. Wickramasinghe, G. Xu, Q. Ye, W. Zhong, Bioorg. Med. Chem. Lett. 20 (2010) 3618–3622.
[14] J.A. Kaizerman, W. Aaron, S. An, R. Austin, M. Brown, A. Chong, T. Huang, R. Hungate, B. Jiang, M.G. Johnson, G. Lee, B.S. Lucas, J. Orf, M. Rong, M.M. Toteva, D. Wickramasinghe, G. Xu, Q. Ye, W. Zhong, D.L. McMinn, Bioorg. Med. Chem. Lett. 20 (2010) 4607–4610.
[15] V.J. Cee, H.L. Deak, B. Du, S.D. Geuns-Meyer, B.L. Hodous, H.N. Nguyen, P.R. Olivieri, V. F. Patel, K. Romero, L. Schenkel, US Patent, 2007, 2007/087276 A1.
[16] M. Payton, T.L. Bush, G. Chung, Cancer Res. 70 (2010) 9846–9854.
[17] V.J. Cee, L.B. Schenkel, B.L. Hodous, H.L. Deak, H.N. Nguyen, P.R. Olivieri, K. Romero, A. Bak, X. Be, S. Bellon, T.L. Bush, A.C. Cheng, G. Chung, S. Coats, P.M. Eden, K. Hanestad, P.L. Gallant, Y. Gu, X. Huang, R.L. Kendall, M.J. Lin, M.J. Morrison, V.F. Patel, R. Radinsky, P.E. Rose, S. Ross, J. Sun, J. Tang, H. Zhao, M. Payton, S.D. Geuns-Meyer, J. Med. Chem. 53 (2010) 6368–6377.
[18] G. Bold, J. Frei, P. Traxler, K.-H. Altmann, H. Mett, D.R. Stover, J.M. Wood, EP Patent, 1998, 98/00764.
[19] G. Bold, K.-H. Altmann, J. Frei, M. Lang, P.W. Manley, P. Traxler, B. Wietfeld, J. Brüggen, E. Buchdunger, R. Cozens, S. Ferrari, P. Furet, F. Hofmann, G. Martiny-Baron, J. Mestan, J. Rösel, M. Sills, D. Stover, F. Acemoglu, E. Boss, R. Emmenegger, L. Lässer, E. Masso, R. Roth, C. Schlachter, W. Vetterli, D. Wyss, J.M. Wood, J. Med. Chem. 43 (2000) 2310–2323.
[20] J. Dumas, J.A. Dixon, Expert Opin. Ther. Pat. 15 (2005) 647–658.
[21] E.L. Piatnitski, M.A.J. Duncton, A.S. Kiselyov, R. Katoch-Rouse, D. Sherman, D.L. Milligan, C. Balagtas, W.C. Wong, J. Kawakamia, J.F. Doody, Bioorg. Med. Chem. Lett. 15 (2005) 4696–4698.
[22] M.A.J. Duncton, E.L. Piatnitski, R. Katoch-Rouse, L.M. Smith, A.S. Kiselyov, D.L. Milligan, C. Balagtas, W.C. Wong, J. Kawakamia, J.F. Doody, Bioorg. Med. Chem. Lett. 16 (2006) 1579–1581.
[23] A.S. Kiselyov, V.V. Semenov, D. Milligan, Chem. Biol. Drug Des. 68 (2006) 308–313.
[24] A.S. Kiselyov, M. Semenova, V.V. Semenov, E.L. Piatnitski, Chem. Biol. Drug Des. 68 (2006) 250–255.
[25] M.A.J. Duncton, E.L.P. Chekler, R. Katoch-Rouse, D. Sherman, W.C. Wong, L.M. Smith, J.K. Kawakami, A.S. Kiselyov, D.L. Milligan, C. Balagtas, Y.R. Hadari, Y. Wang, S.N. Patel, R.L. Rolster, J.R. Tonra, D. Surguladze, S. Mitelman, P. Kussie, P. Bohlen, J.F. Doody, Bioorg. Med. Chem. 17 (2009) 731–740.
[26] J.C. Tille, J. Wood, S.J. Mandriota, C. Schnell, S. Ferrari, J. Mestan, Z. Zhu, L. Witte, M.S. Pepper, J. Pharm. Exp. Ther. 299 (2001) 1073–1085.
[27] G. Papeo, E. Casale, A. Montagnoli, A. Cirla, Expert Opin. Ther. Pat. 23 (2013) 503–514.
[28] V.M. Loh, X.-l. Cockcroft, K.J. Dillon, L. Dixon, J. Drzewiecki, P.J. Eversley, S. Gomez, J. Hoare, F. Kerrigan, I.T.W. Matthews, K.A. Menear, N.M.B. Martin, R.F. Newton, J. Paul, G.C.M. Smith, J. Vilec, A.J. Whittlec, Bioorg. Med. Chem. Lett. 15 (2005) 2235–2238.
[29] X.L. Cockcroft, K.J. Dillon, L. Dixon, J. Drzewiecki, F. Kerrigan, V.M. Loh, N.M.B. Martin, K.A. Menear, G.C.M. Smith, Bioorg. Med. Chem. Lett. 16 (2006) 1040–1044.
[30] K.A. Menear, C. Adcock, R. Boulter, X.-l. Cockcroft, L. Copsey, A. Cranston, K.J. Dillon, J. Drzewiecki, S. Garman, S. Gomez, H. Javaid, F. Kerrigan, C. Knights, A. Lau, V.M. Loh, I.T.W. Matthews, S. Moore, M.J. O'Connor, G.C.M. Smith, N.M.B. Martin, J. Med. Chem. 51 (2008) 6581–6591.
[31] M.E. Prime, S.M. Courtney, F.A. Brookfield, R.W. Marston, V. Walker, J. Warne, A.E. Boyd, N.A. Kairies, W.v.d. Saal, A. Limberg, G. Georges, R.A. Engh, B. Goller, P. Rueger, M. Rueth, J. Med. Chem. 54 (2011) 312–319.

[32] P. Skehan, R. Storeng, D. Scudiero, A. Monks, J. McMahon, D. Vistica, J.T. Warren, H. Bokesch, S. Kenney, M.R. Boyd, J. Natl. Cancer Inst. 82 (1990) 1107–1112.
[33] A. Jemal, F. Bray, M.M. Center, J. Ferlay, E. Ward, D. Forman, CA Cancer. J. Clin. 61 (2011) 69–90.
[34] J.F. Perz, G.L. Armstrong, L.A. Farrington, Y.J.F. Hutin, B.P. Bell, J. Hepatol. 45 (2006) 529–538.
[35] J. Massagué, Nature 432 (2004) 298–306.
[36] Y. Tsujimoto, C.M. Croce, Proc. Natl. Acad. Sci. U. S. A. 83 (1986) 5214–5218.
[37] S. Krajewski, C. Blomqvist, K. Franssila, Cancer Res. 55 (1995) 4471–4478.
[38] S. Haldar, J. Chintapalli, C.M. Croce, Cancer Res. 56 (1996) 1253–1255.
[39] E. Hernández-Núñez, H. Tlahuext, R. Moo-Puc, H. Torres-Gómez, R. Reyes-Martínez, R. Cedillo-Rivera, C. Nava-Zuazo, G. Navarrete-Vazquez, Eur. J. Med. Chem. 44 (2009) 2975–2984.
[40] I.E. Virsis, D.A. Silaraya, B.A. Grinberga, A.A. Prikulis, I.D. Gerbashevska, M.E. Orenish, Khim. Farm. Zh. 15 (1981) 23–26.
[41] Z. Aktürk, F. Kılıç, K. Erol, V. Pabuçcuoğlu, Il Farm. 57 (2002) 201–206.
[42] H.M.B. Cid, C. Tränkle, K. Baumann, R. Pick, E. Mies-Klomfass, E. Kostenis, K. Mohr, U. Holzgrabe, J. Med. Chem. 43 (2000) 2155–2164.
[43] R. Weiss, Org. Syn. Coll. 2 (1943) 61.
[44] P.A. Procopiou, C. Browning, J.M. Buckley, K.L. Clark, L. Fechner, P.M. Gore, A.P. Hancock, S.T. Hodgson, D.S. Holmes, M. Kranz, B.E. Looker, K.M.L. Morriss, D.L. Parton, L.J. Russell, R.J. Slack, S.L. Sollis, S. Vile, C.J. Watts, J. Med. Chem. 54 (2011) 2183–2195.